Measuring the local diffusion coefficient with H.E.S.S. observations of very high-energy electrons

Dan Hooper and Tim Linden

Phys. Rev. D **98**, 083009 — Published 12 October 2018

DOI: 10.1103/PhysRevD.98.083009

FERMILAB-PUB-17-530-A

Prepared for submission to JCAP

Measuring the Local Diffusion Coefficient with H.E.S.S. Observations of Very High-Energy Electrons

Dan Hooper[a,b,c] **and Tim Linden**[d]

[a]Fermi National Accelerator Laboratory, Center for Particle Astrophysics, Batavia, IL 60510
[b]University of Chicago, Department of Astronomy and Astrophysics, Chicago, IL 60637
[c]University of Chicago, Kavli Institute for Cosmological Physics, Chicago, IL 60637
[e]Ohio State University, Center for Cosmology and AstroParticle Physics (CCAPP), Columbus, OH 43210

E-mail: dhooper@fnal.gov, linden.70@osu.edu

Abstract. The HAWC Collaboration has recently reported the detection of bright and spatially extended multi-TeV gamma-ray emission from Geminga, Monogem, and a handful of other nearby, middle-aged pulsars. The angular profile of the emission observed from these pulsars is surprising, in that it implies that cosmic-ray diffusion is significantly inhibited within $\sim$25 pc of these objects, compared to the expectations of standard Galactic diffusion models. This raises the important question of whether the diffusion coefficient in the local interstellar medium is also low, or whether it is instead better fit by the mean Galactic value. Here, we utilize recent observations of the cosmic-ray electron spectrum (extending up to $\sim$20 TeV) by the H.E.S.S. Collaboration to show that the local diffusion coefficient cannot be as low as it is in the regions surrounding Geminga and Monogem. Instead, we conclude that cosmic rays efficiently diffuse through the bulk of the local interstellar medium. Among other implications, this further supports the conclusion that pulsars significantly contribute to the observed positron excess, and provides strong evidence for spatially varying diffusion coefficients throughout the Milky Way.

[1]ORCID: http://orcid.org/0000-0001-8837-4127
[2]ORCID: http://orcid.org/0000-0001-9888-0971

1 Introduction

Measurements of the cosmic-ray positron fraction by the PAMELA [1] and AMS-02 [2] experiments (as well as by HEAT [3], AMS-01 [4] and Fermi [5]) have identified an excess relative to the standard predictions for secondary production in the interstellar medium (ISM). This indicates that significant quantities of ∼0.01-1 TeV positrons must be produced as primary cosmic rays. Because high-energy positrons efficiently cool through a combination of synchrotron and inverse-Compton processes, at least some of these positrons must be produced relatively nearby. Proposals for the origin of these particles include nearby pulsars [6–12], annihilating dark matter [12–25], and the acceleration of secondary positrons in nearby supernova remnants [26–32].

Earlier this year, the scientific collaboration operating the High-Altitude Water Cherenkov (HAWC) Observatory released their first measurements of the very-high energy gamma-ray emission from the nearby pulsars Geminga and Monogem [33] (see also Refs. [34–36]). Even more recently, HAWC has reported that the emission from these sources follows a diffusive profile extending out to at least ∼5° in radius (corresponding to a physical extent of ∼25 pc) [37]. The spatially extended nature of this emission indicates that it is generated through the inverse Compton scattering of very high-energy (VHE) electrons[1] with the cosmic microwave background and other radiation fields. Among other reasons, this result is important because it suggests that HAWC will likely be able to detect the "TeV Halos" around many pulsars, including those whose radio and GeV emission are not beamed in our direction [38]. Furthermore, the collective emission from the TeV Halos associated with the Milky Way's pulsar population is likely to generate much of the VHE gamma-ray emission observed from the Galactic Center [39], as well as the diffuse TeV excess previously reported by Milagro [40].

Interestingly, the fluxes of VHE gamma-rays observed from Geminga and Monogem indicate that these sources inject a flux of positrons into the local ISM that is approximately equal to that required to account for the observed positron excess. Using the results from the HAWC Collaboration's 2HWC catalog [33], we argued previously that this information strongly favors the conclusion that the positron excess is generated by nearby pulsars, diminishing the motivation for annihilating dark matter or other exotic mechanisms [41].

A very different interpretation of this data has recently been put forth by the HAWC Collaboration [37]. The angular profile of the VHE emission observed from Geminga and Monogem indicates that diffusion constant is very low in the regions surrounding these sources, representing the first empirical determination of a diffusion coefficient in a ∼10-50 pc region within the local Galaxy. More quantitatively, they find that their data favors a diffusion coefficient (see Eq. 2.1) for the region surrounding Geminga that is 560^{+260}_{-170} times smaller than the value inferred from measurements of the boron-to-carbon ratio and other cosmic-ray secondary-to-primary ratios (which we take to be the GALPROP default value, $D \approx 3.86 \times 10^{28}\,(E_e/\mathrm{GeV})^{0.33}$ cm^2/s [42]). Similarly, they find that the region surrounding Monogem requires a diffusion coefficient that is smaller than the standard value by a factor of 120^{+180}_{-90}. The authors of Ref. [37] assert that these reduced values for the diffusion coefficient are likely to be indicative of the diffusion coefficient throughout the bulk of the ISM, or at least within a sizable region surrounding the solar position. If true, the flux of cosmic-ray positrons that reaches the Solar System from these and other pulsars would be

[1] Throughout this paper, unless otherwise stated, we refer to both electrons and positrons as simply "electrons".

highly suppressed, suggesting that another – and perhaps more exotic – explanation would be required in order to explain the observed positron excess.

In this paper, we revisit this question and argue that the interpretation put forth in Ref. [37] is incompatible with other cosmic-ray measurements, and in particular with the spectrum of cosmic-ray electrons reported by several experiments, including HESS [43–46], MAGIC [47], AMS-02 [48], VERITAS [49], and Fermi [50]. Of particular interest for the question at hand are the most recent measurements of the cosmic-ray electron spectrum from the HESS Collaboration [46], which extend up to energies as high as ∼20 TeV [46].[2] Because VHE cosmic-ray electrons cool extremely rapidly, they provide critical information regarding the diffusion coefficient in the local ISM. In particular, at 20 TeV, cosmic-ray electrons cool on a timescale of $\sim 10^4$ years. If we adopt a standard value for the diffusion coefficient that is compatible with measurements of the boron-to-carbon and other secondary-to-primary ratios, we estimate that electrons will typically diffuse a distance of $\sim\sqrt{Dt} \sim 200$ pc within this time. However, for the significantly smaller diffusion coefficient advocated in Ref. [37], the horizon for such VHE electrons is reduced to only ∼10–20 pc. As there are no plausible sources of VHE cosmic rays within this radius, we are forced to conclude that diffusion must be reasonably efficient throughout the majority of the local ISM, and that the conditions found in the regions surrounding Geminga and Monogem cannot be representative of the overall local Galactic environment.

2 The Cosmic-Ray Electron Spectrum

The diffusion and energy losses of cosmic-ray electrons can be described by the standard transport equation:

$$\frac{\partial}{\partial t}\frac{dn_e}{dE_e}(E_e,\vec{x},t) = \vec{\bigtriangledown}\cdot\left[D(E_e,\vec{x})\vec{\bigtriangledown}\frac{dn_e}{dE_e}(E_e,\vec{x},t)\right] + \frac{\partial}{\partial E_e}\left[\frac{dE_e}{dt}(E_e)\,\frac{dn_e}{dE_e}(E_e,\vec{x},t)\right] + Q(E_e,\vec{x},t), \tag{2.1}$$

where dn_e/dE_e is the differential number density of electrons, D is the diffusion coefficient, and the source term, Q, describes the spectrum, distribution, and time profile of electrons injected into the ISM. Energy losses from inverse Compton and synchrotron processes are given by [51]:

$$\begin{aligned} -\frac{dE_e}{dt}(r) &= \sum_i \frac{4}{3}\sigma_T \rho_i(r) S_i(E_e)\left(\frac{E_e}{m_e}\right)^2 + \frac{4}{3}\sigma_T \rho_{\rm mag}(r)\left(\frac{E_e}{m_e}\right)^2 \\ &\approx 1.02\times 10^{-16}\,{\rm GeV/s}\,\times\left[\sum_i \frac{\rho_i(r)}{{\rm eV/cm^3}}\,S_i(E_e) + 0.224\left(\frac{B}{3\,\mu{\rm G}}\right)^2\right]\left(\frac{E_e}{\rm GeV}\right)^2, \end{aligned} \tag{2.2}$$

where σ_T is the Thomson cross section and the sum is carried out over the various components of the radiation backgrounds, consisting of the cosmic microwave background (CMB), infrared emission (IR), starlight (star), and ultraviolet emission (UV). Throughout our analysis, we adopt the following parameters: $\rho_{\rm CMB} = 0.260$ eV/cm^3, $\rho_{\rm IR} = 0.60$ eV/cm^3, $\rho_{\rm star} = 0.60$ eV/cm^3, $\rho_{\rm UV} = 0.10$ eV/cm^3, $\rho_{\rm mag} = 0.224$ eV/cm^3 (corresponding to $B = 3\,\mu$G), and $T_{\rm CMB} = 2.7$ K, $T_{\rm IR} = 20$ K, $T_{\rm star} = 5000$ K and $T_{\rm UV}$ =20,000 K. At very high energies

[2] See https://indico.snu.ac.kr/indico/event/15/session/5/contribution/694/material/slides/0.pdf

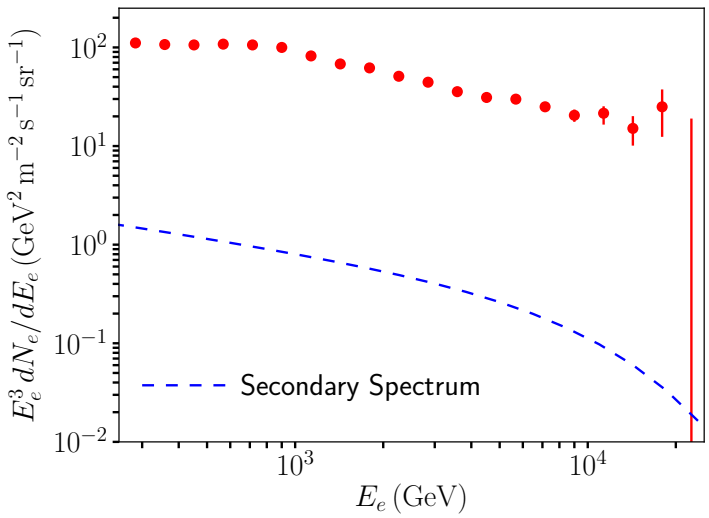

Figure 1. The secondary contribution to the cosmic-ray electron (plus positron) spectrum, as calculated using GALPROP, and adopting the default values for all propagation parameters. Comparing this to the spectrum as reported by the HESS Collaboration, it is clear that secondary production provides only a small fraction of this flux. At the highest measured energies, this result is largely independent of the value of the diffusion coefficient.

($E_e \gtrsim m_e^2/2T$), inverse Compton scattering is suppressed by the following Klein-Nishina factor [52]:

$$S_i(E_e) \approx \frac{45\, m_e^2/64\pi^2 T_i^2}{(45\, m_e^2/64\pi^2 T_i^2) + (E_e^2/m_e^2)}. \tag{2.3}$$

The source term in Eq. 2.1 includes contributions from individual sources of cosmic-ray electrons (pulsars, supernova remnants, etc.), as well as from the production of secondary particles. Secondary electrons and positrons are generated in the decays of pions and kaons that are produced in the collisions of hadronic cosmic rays with gas. The flux of cosmic-ray secondaries can be calculated from Eq. 2.1 by setting $Q = \int J_p n_{\rm gas} (d\sigma/dE) dE_p$, where J_p is the flux of hadronic cosmic rays, $n_{\rm gas}$ the gas density, and $d\sigma/dE$ is the differential cross section for the production of electrons and positrons [53].

At the highest measured energies, cosmic-ray electrons cool on a timescale of $\sim 3 \times 10^4$ years $\times$ (10 TeV/E_e), during which they diffuse a distance of only $\sim \sqrt{Dt} \sim 300$ pc (for the diffusion coefficient inferred from measurements of the boron-to-carbon and other cosmic-ray secondary-to-primary ratios, $D \approx 3.86 \times 10^{28}\, (E_e/\mathrm{GeV})^{0.33}$ cm^2/s). In light of this, only a small volume contributes to the local VHE electron spectrum. Over this volume, the densities of both hadronic cosmic rays and gas are reasonably well known, allowing us to fairly reliably calculate the flux of VHE secondaries. Reducing the value of the diffusion coefficient will not substantially impact the local flux of VHE secondaries, because the cosmic-ray proton density is roughly homogeneous within this region.

In Fig. 1 we plot the spectrum of secondary electrons as predicted using the publicly available code GALPROP [42]. Here we have adopted the default parameter values, including a diffusion coefficient of $D = 3.86 \times 10^{28}\, (E_e/\mathrm{GeV})^{0.33}$ cm^2/s. From this figure, it is clear that flux of secondaries is quite small, making up only $\sim$1% of the measured cosmic-ray electron spectrum. We thus conclude that secondaries contribute negligibly to the measured

electron spectrum, especially at the highest measured energies. We note that the secondary contribution to the total electron spectrum near Earth is likely to be even lower than predicted by our GALPROP model – because we reside in a void (known as the local bubble), which contains an average gas density more than an order of magnitude below the average value for the galactic plane. Our GALPROP model, which is axisymmetric, does not model this local feature, and thus overpredicts the local secondary electron and positron production rate. This strong constraint on secondary production provides the first indication that a significant flux of ∼20 TeV primary electrons are produced in close proximity to the Solar System.

Next, we calculate the contribution to the cosmic-ray electron spectrum from individual nearby sources. In the top frame of Fig. 2, we plot the spectral shape (arbitrarily normalized) of cosmic-ray electrons from a source located at distances between 200 and 1000 pc, for a standard diffusion coefficient of $D = 3.86 \times 10^{28}\,(E_e/\mathrm{GeV})^{0.33}$ cm^2/s. For the spectrum that is injected from these sources, we have adopted a power-law form, $dN_e/dE_e \propto E^{-\alpha}$, with an index of $\alpha = 2$. It is clear from this figure that the observed spectrum requires the presence of sources within approximately ∼500 pc of the Solar System, at least for this choice of the diffusion coefficient and spectral index.

In the lower frame of Fig. 2, we show the primary electron spectrum generated by a source that is located only 200 pc from the Solar System, assuming a significantly lower diffusion coefficient of $D = 3.86 \times 10^{26}\,(E_e/\mathrm{GeV})^{0.33}$ cm^2/s, as advocated by the HAWC Collaboration.[3] These results indicate that, if the local ISM were described by such a low diffusion coefficient, the nearest known high-energy sources would be unable to explain the HESS electron flux above ∼1-2 TeV, even if the source spectrum were as hard as $\alpha = 1$. This is our primary argument explaining why cosmic-rays propagating throughout the bulk of the local ISM cannot be as strongly confined as implied by HAWC's observations of Geminga and Monogem. These observed TeV halos must instead occupy unusual regions, distinct from the majority of the local ISM.

Finally, we consider a simple but realistic distribution of cosmic-ray sources in order to demonstrate that the observed electron spectrum can be easily understood within the context of conventional diffusion models, such as those long-favored by the boron-to-carbon ratio and other measurements. We adopt a distribution of cosmic-ray sources that is described by a Lorimer profile [54] with an exponential disk:

$$n_{\mathrm{sources}} \propto R^{2.35}\,\exp(-R/1530\,\mathrm{pc})\,\exp(-|z|/300\,\mathrm{pc}). \tag{2.4}$$

Here R and z describe the Galaxy in cylindrical coordinates. We also adopt an injected spectral index of $\alpha = 2$ and a standard diffusion coefficient of $D = 3.86 \times 10^{28}\,(E_e/\mathrm{GeV})^{0.33}$ cm^2/s. In Fig. 3, the black dashed line denotes the contribution from the portion of this source population that is located at more than 0.8 kpc from the Solar System, which we assume to be in steady-state. From this figure, it is clear that such a population can account for the observed cosmic-ray electron spectrum up to ∼3 TeV. At higher energies, however, local sources must play an important role.

With this in mind, we additionally show the contributions to the cosmic-ray electron spectrum from the Geminga (dashed green) and Monogem (dot-dashed black) pulsars, adopting ages and distances for these sources of 370 and 110 kyr, and 250 and 280 pc, respectively.

[3] Throughout, we have adopted a maximum injected energy of 1 PeV. Although most of our results are not sensitive to this choice, the case in which $\alpha = 1$ (in the lower frame of Fig. 2) is an exception.

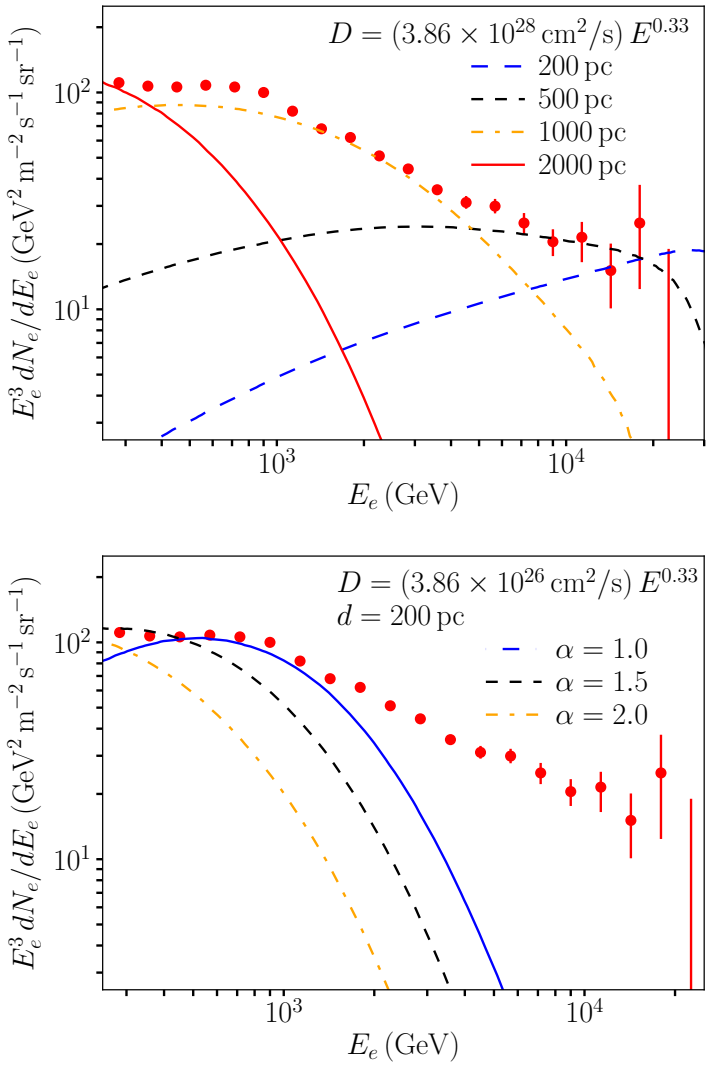

Figure 2. The contribution to the cosmic-ray electron (plus positron) spectrum from individual nearby sources. In the top frame we plot the spectrum (arbitrarily normalized) of cosmic-ray electrons from a source located at various distances for a standard diffusion coefficient of $D = 3.86 \times 10^{28}\,(E_e/\mathrm{GeV})^{0.33}$ cm^2/s and an injected spectral index of $\alpha = 2$. In the lower frame, we plot the spectrum from a source 200 pc from the Solar System with a much lower diffusion coefficient in the range favored by HAWC for the regions surrounding the Geminga and Monogem, $D = 3.86 \times 10^{26}\,(E_e/\mathrm{GeV})^{0.33}$ cm^2/s. If the ISM were described by such a low diffusion coefficient, this figure demonstrates that even very nearby sources could not account for the electron spectrum observed above ∼1-2 TeV. This is our main argument for why cosmic-ray confinement throughout the bulk of the ISM cannot be as efficient as has been observed by HAWC in the regions surrounding Geminga and Monogem.

For these individual systems, we have assumed a time-dependent emission intensity that is proportional to the spin-down power of the pulsar, $L_e \propto [1 + (t/\tau)]^{-2}$, where we have chosen a spin-down timescale of $\tau = 10^4$ years [55]. In each case, we have normalized the emission to 30% of the pulsars' total spindown power and have adopted an injected spectral index of $\alpha = 2$. We note that the injected spectrum of $\alpha = 2$ is somewhat softer than the $1.5 < \alpha < 1.9$

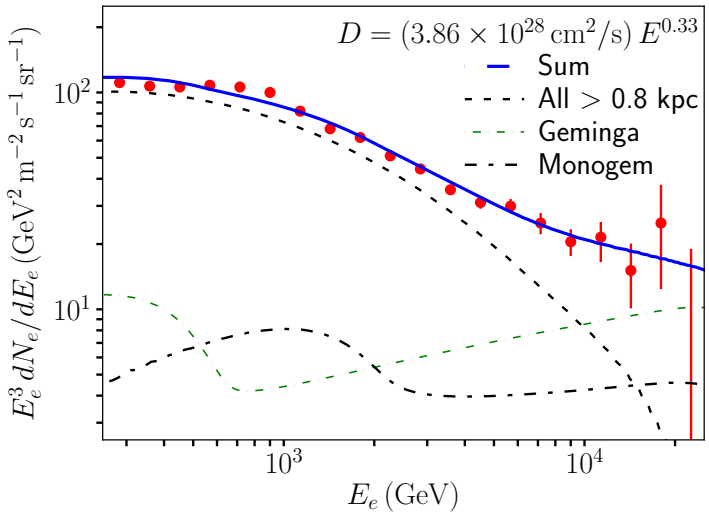

Figure 3. The contribution to the cosmic-ray electron (plus positron) spectrum from all sources more than 800 pc from the Solar System (dashed black), and from the Geminga (dashed green) and Monogem (dot-dashed black) pulsars. Here we had adopted a distribution of sources with a scale height of 300 pc, injected spectral indices of $\alpha = 2$, pulsar spindown timescales of $\tau = 10^4$ years, and a diffusion coefficient of $D = 3.86 \times 10^{28}\,(E_e/\mathrm{GeV})^{0.33}$ cm^2/s. This collection of sources can easily account for the cosmic-ray electron spectrum as measured by HESS and other experiments, while scenarios with a much lower diffusion coefficient cannot.

spectrum necessary to fit the gamma-ray emission spectrum observed by HAWC from these sources [41]. However, this softened spectrum approximately takes into account the additional electron cooling which occurs within the TeV halo before these electrons escape into the surrounding ISM. The sum of the contributions from these two sources and that from the population of more distant sources can easily account for the spectrum that has been reported by HESS and other experiments. In contrast, if we adopt a diffusion coefficient that is ∼100-500 times lower (as argued in Ref. [37]), it is not possible to account for the cosmic-ray electron spectrum observed above ∼1-2 TeV.

3 Discussion and Summary

Recent observations by the HAWC Collaboration of the very high-energy (VHE) gamma-ray emission from the Geminga and Monogem pulsars indicate that cosmic rays diffuse very slowly in the regions immediately surrounding these objects. The HAWC Collaboration has recently interpreted these measurements as evidence for a very low diffusion coefficient throughout the local interstellar medium (ISM) [37], approximately ∼100-500 times smaller than the value long-inferred from measurements of boron-to-carbon and other secondary-to-primary ratios in the cosmic-ray spectrum. If this were the case, the positron excess as reported by PAMELA [1] and AMS-02 [2] could not be accounted for by pulsars, motivating more exotic explanations.

If the value of the local diffusion coefficient were as low as advocated by the HAWC Collaboration, some exotic mechanism would be required in order to produce the observed positron excess. In such a scenario, we point out that this mechanism, or a second exotic mechanism, would also be required to produce the measured spectrum of VHE electrons.

Such scenarios are very strongly constrained, however. For the case of annihilating dark matter, for example, gamma-ray observations of dwarf spheroidal galaxies by the Fermi-LAT Collaboration have already ruled out the vast majority of dark matter models that are potentially capable of generating the observed positron excess [56–58]. Furthermore, the rapid cooling times of ∼20 TeV electrons require even more massive dark matter particles, with significantly higher annihilation rates. Gamma-ray constraints thus extremely strongly disfavor dark matter interpretations of the VHE cosmic-ray electron spectrum.

In this paper, we have argued that another interpretation of this data is much more likely. In particular, we have demonstrated that the cosmic-ray electron spectrum as measured by several experiments including HESS [46] is incompatible with scenarios in which transport through the ISM is described by a diffusion coefficient that is as low as suggested by the HAWC Collaboration [37]. More specifically, with such efficient cosmic-ray confinement, the highest energy electrons currently observed by HESS (∼20 TeV) would only travel ∼10-20 pc before losing their energy. Given that no plausible sources of VHE cosmic rays exist within this radius, one must conclude that transport throughout the bulk of the ISM is described by a substantially larger diffusion coefficient.

HAWC's observations inform us as to the diffusion coefficient within approximately ∼25 pc around Geminga and Monogem, but provide no direct information about diffusion in the remaining bulk of the ISM. We argue here that it is very likely that the conditions that dictate cosmic-ray diffusion around Geminga and B0656+14 are very different from those found elsewhere in the ISM – that is, we argue that the diffusion coefficient throguhout the galaxy is inhomogeneous. Recently, similar conclusions have been reached by two outside groups, who additionally produce quantitative models that divide the galactic diffusion constant into two regions. Among other results, these models empirically show that positrons may escape from low-diffusion regions near the Geminga TeV halo and subsequently propagate efficiently towards Earth, providing an explanation for the high-energy positron excess [59, 60].

Intriguingly, previous work has suggested that cosmic-ray gradients can produce regions of inhibited diffusion near supernova remnants on much smaller distance scales [61–66]. Very recently, it has been proposed that an analogous mechanism may be active in regions near young pulsars [67]. Studies of supernova remnants also indicate that local diffusion constants may be highly anisotropic, which may significantly impact the calculated diffusion coefficients in this region [68]. However, HAWC observations of the Geminga TeV halo indicate that it is approximately spherically symmetric, reducing the need for an anisotropic diffusion tensor [37]. Regardless of the mechanism that produces the inhibited diffusion, it is clear that the complex magnetic field structure necessary to contain charged cosmic-rays within TeV halos may provide significant clues regarding the structure of the interstellar medium [69]. Further studies are necessary to understand the formation and evolution of magnetic fields near energetic leptonic sources.

Here, we only note that empircal studies of galactic cosmic-ray propagation can place constraints on the extent of these cosmic-ray confinement regions. If all, or most, young and middle-aged pulsars are surrounded by a region with efficient cosmic-ray confinement ($D \ll D_{\rm ISM}$), the volume of such regions must be fairly small in order to avoid conflicting with measurements of boron-to-carbon and other secondary-to-primary ratios. In particular, if such regions have a typical radius of $r_{\rm region}$, then they will collectively occupy roughly the

following fraction of the volume of the Milky Way's disk: [41]

$$f \sim \frac{N_{\rm region} \times \frac{4\pi}{3} r_{\rm region}^3}{\pi R_{\rm MW}^2 \times 2 z_{\rm MW}} \tag{3.1}$$
$$\sim 0.007 \times \left(\frac{r_{\rm region}}{30\,{\rm pc}}\right)^3 \left(\frac{\dot{N}_{\rm SN}}{0.03\,{\rm yr}^{-1}}\right) \left(\frac{\tau_{\rm region}}{10^6\,{\rm yr}}\right) \left(\frac{20\,{\rm kpc}}{R_{\rm MW}}\right)^2 \left(\frac{200\,{\rm pc}}{z_{\rm MW}}\right),$$

where $\dot{N}_{\rm SN}$ is the rate at which new pulsars appear in the Galaxy, $\tau_{\rm region}$ is the length of time that such regions persist, and $N_{\rm region} = \dot{N}_{\rm SN} \times \tau_{\rm region}$ is the number of such regions present at a given time. The quantities $R_{\rm MW}$ and $z_{\rm MW}$ denote the radius and half-width of the Galaxy's cylindrical disk. For such a small fraction of the total volume of the ISM, we expect such regions to have little impact on the observed secondary-to-primary ratios. In contrast, if most of such regions were as large as $r_{\rm region} \sim 150$ pc or greater, they would collectively occupy most of the ISM and dramatically impact cosmic-ray transport throughout the Milky Way.

Lastly, we would like to emphasize that we are not arguing in this paper that the diffusion coefficient is entirely uniform or homogeneous throughout the Milky Way's ISM. Some variation is, of course, almost certain to exist. It has even been shown that the measured spectra of cosmic-ray protons, antiprotons and helium nuclei prefer somewhat different propagation parameters than those which provide the best-fit to the observed ratios of heavier nuclei (Be, B, C, N, O). This suggests that different cosmic-ray species may be probing different regions of the ISM, with different physical characteristics [70]. Additionally, it is possible that the diffusion coefficient is anisotropic, especially near sources [68]. In this case, the diffusion coefficients quoted throughout this work are simply the best-fitting spherical approximation to a more complex diffusion tensor. These differences, however, are much more modest than those being argued for in Ref. [37], typically affecting cosmic-ray confinement by tens of percents rather than factors of ∼100-500. The fact that the spectrum of each of these cosmic-ray species favors similar (if not identical) diffusion parameters to those shown here to be favored by the cosmic-ray electron spectrum provides considerable evidence for approximately homogeneous diffusion throughout the bulk of the Milky Way's ISM.

In Summary, the observations by HAWC and Milagro have revealed that the pulsars Geminga and Monogem are surrounded by regions in which cosmic-ray confinement is extremely efficient, featuring diffusion coefficients that are hundreds of times smaller than those determined by boron-to-carbon and other cosmic-ray secondary-to-primary ratios. Here we have argued, however, that these regions must be of quite limited size, and that diffusion must be significantly more effective throughout the majority of the local ISM. In particular, we show that the VHE electron spectrum can only be explained (without the presence of extremely nearby sources, $d \lesssim 20$ pc) if the local diffusion coefficient is more similar to the value long-inferred from boron-to-carbon and other cosmic ray measurements than to that recently advocated for by the HAWC Collaboration.

Acknowledgments. DH is supported by the US Department of Energy under contract DE-FG02-13ER41958. Fermilab is operated by Fermi Research Alliance, LLC, under contract DE- AC02-07CH11359 with the US Department of Energy. TL acknowledges support from NSF Grant PHY-1404311.

References

[1] PAMELA collaboration, O. Adriani et al., *PAMELA results on the cosmic-ray antiproton flux from 60 MeV to 180 GeV in kinetic energy*, *Phys. Rev. Lett.* **105** (2010) 121101, [1007.0821].

[2] AMS collaboration, M. Aguilar et al., *First Result from the Alpha Magnetic Spectrometer on the International Space Station: Precision Measurement of the Positron Fraction in Primary Cosmic Rays of 0.5350 GeV*, *Phys. Rev. Lett.* **110** (2013) 141102.

[3] HEAT collaboration, S. W. Barwick et al., *Measurements of the cosmic ray positron fraction from 1-GeV to 50-GeV*, *Astrophys. J.* **482** (1997) L191–L194, [astro-ph/9703192].

[4] AMS 01 collaboration, M. Aguilar et al., *Cosmic-ray positron fraction measurement from 1 to 30-GeV with AMS-01*, *Phys. Lett.* **B646** (2007) 145–154, [astro-ph/0703154].

[5] Fermi-LAT collaboration, M. Ackermann et al., *Measurement of separate cosmic-ray electron and positron spectra with the Fermi Large Area Telescope*, *Phys. Rev. Lett.* **108** (2012) 011103, [1109.0521].

[6] D. Hooper, P. Blasi and P. D. Serpico, *Pulsars as the Sources of High Energy Cosmic Ray Positrons*, *JCAP* **0901** (2009) 025, [0810.1527].

[7] H. Yuksel, M. D. Kistler and T. Stanev, *TeV Gamma Rays from Geminga and the Origin of the GeV Positron Excess*, *Phys. Rev. Lett.* **103** (2009) 051101, [0810.2784].

[8] S. Profumo, *Dissecting cosmic-ray electron-positron data with Occam's Razor: the role of known Pulsars*, *Central Eur. J. Phys.* **10** (2011) 1–31, [0812.4457].

[9] D. Malyshev, I. Cholis and J. Gelfand, *Pulsars versus Dark Matter Interpretation of ATIC/PAMELA*, *Phys. Rev.* **D80** (2009) 063005, [0903.1310].

[10] Fermi-LAT collaboration, D. Grasso et al., *On possible interpretations of the high energy electron-positron spectrum measured by the Fermi Large Area Telescope*, *Astropart. Phys.* **32** (2009) 140–151, [0905.0636].

[11] T. Linden and S. Profumo, *Probing the Pulsar Origin of the Anomalous Positron Fraction with AMS-02 and Atmospheric Cherenkov Telescopes*, *Astrophys.J.* **772** (2013) 18, [1304.1791].

[12] I. Cholis and D. Hooper, *Dark Matter and Pulsar Origins of the Rising Cosmic Ray Positron Fraction in Light of New Data From AMS*, *Phys. Rev.* **D88** (2013) 023013, [1304.1840].

[13] L. Bergstrom, T. Bringmann and J. Edsjo, *New Positron Spectral Features from Supersymmetric Dark Matter - a Way to Explain the PAMELA Data?*, *Phys. Rev.* **D78** (2008) 103520, [0808.3725].

[14] M. Cirelli and A. Strumia, *Minimal Dark Matter predictions and the PAMELA positron excess*, *PoS* **IDM2008** (2008) 089, [0808.3867].

[15] I. Cholis, L. Goodenough, D. Hooper, M. Simet and N. Weiner, *High Energy Positrons From Annihilating Dark Matter*, *Phys. Rev.* **D80** (2009) 123511, [0809.1683].

[16] M. Cirelli, M. Kadastik, M. Raidal and A. Strumia, *Model-independent implications of the e+-, anti-proton cosmic ray spectra on properties of Dark Matter*, *Nucl. Phys.* **B813** (2009) 1–21, [0809.2409].

[17] A. E. Nelson and C. Spitzer, *Slightly Non-Minimal Dark Matter in PAMELA and ATIC*, *JHEP* **10** (2010) 066, [0810.5167].

[18] N. Arkani-Hamed, D. P. Finkbeiner, T. R. Slatyer and N. Weiner, *A Theory of Dark Matter*, *Phys. Rev.* **D79** (2009) 015014, [0810.0713].

[19] I. Cholis, D. P. Finkbeiner, L. Goodenough and N. Weiner, *The PAMELA Positron Excess from Annihilations into a Light Boson*, *JCAP* **0912** (2009) 007, [0810.5344].

[20] I. Cholis, G. Dobler, D. P. Finkbeiner, L. Goodenough and N. Weiner, *The Case for a 700+ GeV WIMP: Cosmic Ray Spectra from ATIC and PAMELA*, *Phys. Rev.* **D80** (2009) 123518, [0811.3641].

[21] R. Harnik and G. D. Kribs, *An Effective Theory of Dirac Dark Matter*, *Phys. Rev.* **D79** (2009) 095007, [0810.5557].

[22] P. J. Fox and E. Poppitz, *Leptophilic Dark Matter*, *Phys. Rev.* **D79** (2009) 083528, [0811.0399].

[23] M. Pospelov and A. Ritz, *Astrophysical Signatures of Secluded Dark Matter*, *Phys. Lett.* **B671** (2009) 391–397, [0810.1502].

[24] J. D. March-Russell and S. M. West, *WIMPonium and Boost Factors for Indirect Dark Matter Detection*, *Phys. Lett.* **B676** (2009) 133–139, [0812.0559].

[25] S. Chang and L. Goodenough, *Charge Asymmetric Cosmic Ray Signals From Dark Matter Decay*, *Phys. Rev.* **D84** (2011) 023524, [1105.3976].

[26] P. Blasi, *The origin of the positron excess in cosmic rays*, *Phys. Rev. Lett.* **103** (2009) 051104, [0903.2794].

[27] P. Mertsch and S. Sarkar, *Testing astrophysical models for the PAMELA positron excess with cosmic ray nuclei*, *Phys. Rev. Lett.* **103** (2009) 081104, [0905.3152].

[28] M. Ahlers, P. Mertsch and S. Sarkar, *On cosmic ray acceleration in supernova remnants and the FERMI/PAMELA data*, *Phys. Rev.* **D80** (2009) 123017, [0909.4060].

[29] I. Cholis and D. Hooper, *Constraining the origin of the rising cosmic ray positron fraction with the boron-to-carbon ratio*, *Phys. Rev.* **D89** (2014) 043013, [1312.2952].

[30] M. Kachelriess, S. Ostapchenko and R. Tomas, *Antimatter production in supernova remnants*, *Astrophys. J.* **733** (2011) 119, [1103.5765].

[31] M. Kachelrie and S. Ostapchenko, *B/C ratio and the PAMELA positron excess*, *Phys. Rev.* **D87** (2013) 047301, [1211.1033].

[32] I. Cholis, D. Hooper and T. Linden, *Evidence for the Stochastic Acceleration of Secondary Antiprotons by Supernova Remnants*, 1701.04406.

[33] A. U. Abeysekara et al., *The 2HWC HAWC Observatory Gamma Ray Catalog*, 1702.02992.

[34] B. M. Baughman, J. Wood and for the HAWC Collaboration, *TeV Gamma-Ray Emission Observed from Geminga with HAWC*, *ArXiv e-prints* (Aug., 2015) , [1508.03497].

[35] A. Carramiñana, *First year results of the High Altitude Water Cherenkov observatory*, in *Journal of Physics Conference Series*, vol. 761 of *Journal of Physics Conference Series*, p. 012034, Oct., 2016. 1609.01768. DOI.

[36] J. Pretz and for the HAWC Collaboration, *Highlights from the High Altitude Water Cherenkov Observatory*, *ArXiv e-prints* (Sept., 2015) , [1509.07851].

[37] A. U. Abeysekara et al., *Extended gamma-ray sources around pulsars constrain the origin of the positron flux at Earth*, 1711.06223.

[38] T. Linden, K. Auchettl, J. Bramante, I. Cholis, K. Fang, D. Hooper et al., *Using HAWC to Discover Invisible Pulsars*, *Submitted to: Phys. Rev. D* (2017) , [1703.09704].

[39] D. Hooper, I. Cholis and T. Linden, *TeV Gamma Rays From Galactic Center Pulsars*, 1705.09293.

[40] T. Linden and B. J. Buckman, *Pulsar TeV Halos Explain the TeV Excess Observed by Milagro*, 1707.01905.

[41] D. Hooper, I. Cholis, T. Linden and K. Fang, *HAWC Observations Strongly Favor Pulsar Interpretations of the Cosmic-Ray Positron Excess*, *Phys. Rev. D, in press* (2017) ,

[1702.08436].

[42] http://galprop.stanford.edu/.

[43] H.E.S.S. collaboration, F. Aharonian et al., *The energy spectrum of cosmic-ray electrons at TeV energies*, *Phys. Rev. Lett.* **101** (2008) 261104, [0811.3894].

[44] H.E.S.S. collaboration, F. Aharonian et al., *Probing the ATIC peak in the cosmic-ray electron spectrum with H.E.S.S*, *Astron. Astrophys.* **508** (2009) 561, [0905.0105].

[45] H.E.S.S. collaboration, H. Abdalla et al., *Contributions of the High Energy Stereoscopic System (H.E.S.S.) to the 35th International Cosmic Ray Conference (ICRC), Busan, Korea*, 2017. 1709.06442.

[46] H.E.S.S. collaboration, D. Kerszberg, M. Kraus, D. Kolitzus, K. Egberts, S. Funk, J. Lenain et al., *The cosmic-ray electron spectrum measured with H.E.S.S.*, in *Talk at the 35th International Cosmic Ray Conference (ICRC), Busan, Korea*, 2017.

[47] MAGIC collaboration, D. Borla Tridon, P. Colin, L. Cossio, M. Doro and V. Scalzotto, *Measurement of the cosmic electron spectrum with the MAGIC telescopes*, in *Proceedings, 32nd International Cosmic Ray Conference (ICRC 2011): Beijing, China, August 11-18, 2011*, vol. 6, pp. 47–50, 2011. 1110.4008. DOI.

[48] AMS collaboration, M. Aguilar et al., *Precision Measurement of the $(e^+ + e)$ Flux in Primary Cosmic Rays from 0.5 GeV to 1 TeV with the Alpha Magnetic Spectrometer on the International Space Station*, *Phys. Rev. Lett.* **113** (2014) 221102.

[49] VERITAS collaboration, D. Staszak, *A Cosmic-ray Electron Spectrum with VERITAS*, *PoS* **ICRC2015** (2016) 411, [1508.06597].

[50] Fermi-LAT collaboration, S. Abdollahi et al., *Cosmic-ray electron-positron spectrum from 7 GeV to 2 TeV with the Fermi Large Area Telescope*, *Phys. Rev.* **D95** (2017) 082007, [1704.07195].

[51] G. R. Blumenthal and R. J. Gould, *Bremsstrahlung, synchrotron radiation, and compton scattering of high-energy electrons traversing dilute gases*, *Rev. Mod. Phys.* **42** (1970) 237–270.

[52] M. S. Longair, *High Energy Astrophysics. Third Edition.* 2011.

[53] I. V. Moskalenko and A. W. Strong, *Production and propagation of cosmic ray positrons and electrons*, *Astrophys. J.* **493** (1998) 694–707, [astro-ph/9710124].

[54] D. R. Lorimer, *The galactic population and birth rate of radio pulsars*, astro-ph/0308501.

[55] B. M. Gaensler and P. O. Slane, *The evolution and structure of pulsar wind nebulae*, *Ann. Rev. Astron. Astrophys.* **44** (2006) 17–47, [astro-ph/0601081].

[56] A. Geringer-Sameth, S. M. Koushiappas and M. G. Walker, *A Comprehensive Search for Dark Matter Annihilation in Dwarf Galaxies*, 1410.2242.

[57] Fermi-LAT collaboration, M. Ackermann et al., *Searching for Dark Matter Annihilation from Milky Way Dwarf Spheroidal Galaxies with Six Years of Fermi-LAT Data*, 1503.02641.

[58] DES, Fermi-LAT collaboration, A. Albert et al., *Searching for Dark Matter Annihilation in Recently Discovered Milky Way Satellites with Fermi-LAT*, *Astrophys. J.* **834** (2017) 110, [1611.03184].

[59] K. Fang, X.-J. Bi, P.-F. Yin and Q. Yuan, *Two-zone diffusion of electrons and positrons from Geminga explains the positron anomaly*, *Astrophys. J.* **863** (2018) 30, [1803.02640].

[60] S. Profumo, J. Reynoso-Cordova, N. Kaaz and M. Silverman, *Lessons from HAWC pulsar wind nebulae observations: The diffusion constant is not a constant; pulsars remain the likeliest sources of the anomalous positron fraction; cosmic rays are trapped for long periods of time in pockets of inefficient diffusion*, *Phys. Rev.* **D97** (2018) 123008, [1803.09731].

[61] A. Achterberg, *The ponderomotive force due to cosmic ray generated Alfven waves*, A&A **98** (May, 1981) 195–197.

[62] V. S. Ptuskin, V. N. Zirakashvili and A. A. Plesser, *Non-linear diffusion of cosmic rays*, *Advances in Space Research* **42** (Aug., 2008) 486–490.

[63] M. A. Malkov, P. H. Diamond, R. Z. Sagdeev, F. A. Aharonian and I. V. Moskalenko, *Analytic Solution for Self-regulated Collective Escape of Cosmic Rays from Their Acceleration Sites*, ApJ **768** (May, 2013) 73, [1207.4728].

[64] M. D'Angelo, P. Blasi and E. Amato, *Grammage of cosmic rays around Galactic supernova remnants*, *Phys. Rev.* **D94** (2016) 083003, [1512.05000].

[65] L. Nava, S. Gabici, A. Marcowith, G. Morlino and V. S. Ptuskin, *Non-linear diffusion of cosmic rays escaping from supernova remnants - I. The effect of neutrals*, MNRAS **461** (Oct., 2016) 3552–3562, [1606.06902].

[66] M. D'Angelo, G. Morlino, E. Amato and P. Blasi, *Diffuse gamma-ray emission from self-confined cosmic rays around Galactic sources*, 1710.10937.

[67] C. Evoli, T. Linden and G. Morlino, *Self-Generated Cosmic-Ray Confinement in TeV Halos: Implications for TeV Gamma-Ray Emission and the Positron Excess*, 1807.09263.

[68] L. Nava and S. Gabici, *Anisotropic cosmic ray diffusion and gamma-ray production close to supernova remnants, with an application to W28*, MNRAS **429** (Feb., 2013) 1643–1651, [1211.1668].

[69] R. Lpez-Coto and G. Giacinti, *Constraining the properties of the magnetic turbulence in the Geminga region using HAWC γ-ray data*, *Mon. Not. Roy. Astron. Soc.* **479** (2018) 4526, [1712.04373].

[70] G. Jhannesson et al., *Bayesian analysis of cosmic-ray propagation: evidence against homogeneous diffusion*, *Astrophys. J.* **824** (2016) 16, [1602.02243].